Physicochemical and dissolution properties of ezetimibe–aspirin binary system in development of fixed-dose combinations

Agata Górniak[1] · Hanna Czapor-Irzabek[1] · Adrianna Złocińska[1] · Bożena Karolewicz[2]

Abstract

The objective of this work was to investigate binary pharmaceutical mixtures of ezetimibe (EZT) and aspirin (ASA) in order to identify whether the occurrence of eutectic in this system has an effect on EZT dissolution improvement. Ezetimibe–aspirin (EZT–ASA) solid dispersions prepared by grinding in the whole range of compositions were characterized using differential scanning calorimetry (DSC) for purpose to describe solid-liquid phase equilibrium diagram. The occurrence of interactions between ingredients was excluded by Fourier transform infrared spectroscopy and X-ray powder diffractometry. Dissolution studies have shown that the mixtures containing from 10 to 60 mass% of EZT (53.5 mass% of EZT in eutectic composition) have released ezetimibe faster than a sample of pure drug. Moreover, ASA is released more quickly from all obtained dispersions than from powder alone. Our studies have shown that obtained mixtures are useful to obtain the fixed-dose combinations, capable to deliver these two APIs together in a single system with enhanced dissolution of EZT and ASA.

Keywords Ezetimibe · Aspirin · DSC · Eutectic · Dissolution · Fixed-dose

Introduction

Cardiovascular diseases (CVD) are recognized as the most common causes of death in the world [1]. It is well known that cholesterol deposition in the arterial wall leads to atherosclerosis, as well as elevated levels of blood lipids are one of the main risk factors of CVD [2]. According to the recommendations of international guidelines, to reduce the risk of a recurrent non-fatal or fatal cardiovascular disease, patients who have had a heart attack or ischaemic stroke should take a long-term combination of multiple pills, or a fixed-dose combination of antiplatelet agent, lipid-lowering agents and blood pressure lowering drugs [3, 4]. The use of fixed-dose combination products allows to concomitantly reduce multiple cardiovascular (CV) risk factors without increasing the pill burden or the risk of adverse effects [5, 6]. The development of effective therapeutic strategies

for the treatment of dyslipidaemia includes the design of new drug forms containing two or more APIs with various pharmacological activities [7–9]. The combination of different drugs in a single pharmaceutical dosage form may have an effect on the physicochemical properties of each and every individual component [10]. Most of the active pharmaceutical ingredients (APIs) used in treatment of lipid disorders like simvastatin, lovastatin and fenofibrate are characterized by low water solubility and, as a result of slow release, have limited oral bioavailability. Ezetimibe, due to low solubility and high permeability, also belongs to II class of BCS (Biopharmaceutics Classification System) [11]. It is the first known hypolipidemic drug that selectively inhibits absorption of dietary and biliary cholesterol in the small intestine [12, 13]. The efficacy of ezetimibe was evaluated by Knopp et al. in 2001 in studies involving patients with primary hypercholesterolaemia [14]. Ezetimibe (EZT) is often added to lipid-lowering therapy, when statins are insufficient to reach recommended LDL-C goals [15]. Ezetimibe monotherapy is recommended as an option for treating patients with primary hypercholesterolaemia (heterozygous familial and non-familial) in whom statins were contraindicated or were statin-intolerant [16, 17]. Acetylsalicylic acid, commonly known by its commercial name aspirin (ASA), is the most commonly prescribed antiplatelet

✉ Agata Górniak
agata.gorniak@umed.wroc.pl

1 Laboratory of Elemental Analysis and Structural Research, Wroclaw Medical University, Borowska 211A, 50-556, Wroclaw, Poland

2 Department of Drug Form Technology, Wroclaw Medical University, Borowska 211A, 50-556, Wroclaw, Poland

drug used in the prevention of arterial thrombogenesis to reduce the risk of myocardial infarction and thrombotic stroke [18, 19]. Low-dose aspirin therapy is recommended for secondary prevention of CV events. Current guidelines define also a role for aspirin in CV primary prevention [4]. Our previous studies have shown that ASA as a second component in the drug–drug binary mixtures positively affects the dissolution rate of components. So that binary mixtures of fenofibrate/aspirin, simvastatin/aspirin and lovastatin/aspirin are characterized by an increased dissolution rate of fenofibrate, simvastatin or lovastatin, observed at the eutectic formation region [20–22]. Although simple combinations of EZT–ASA have not yet been described, many studies emphasize that co-administration of two active pharmaceutical ingredients in one dosage form in comparison with the administration of two single tablets could increase patient compliance, which is the goal in the therapy of cardiovascular diseases [8, 23]. There are reported many studies relating to drug formulations containing EZT or ASA alone. A suitable pharmaceutical composition capable of delivering these two APIs together in a single system with enhanced dissolution is still lacking.

The preparation of drug–drug eutectic mixture [24, 25], which is classified as a crystalline solid dispersion (first generation of solid dispersions) [26], is a promising method for improving the aqueous solubility of its components. The purpose of this study was to evaluate the physicochemical properties of binary pharmaceutical compositions of EZT and ASA to identify whether the occurrence of an eutectic mixture can enhance solubility and dissolution rate for these APIs.

Experimental

Materials

Ezetimibe was donated by the Pharmaceutical Research Institute (Poland). Acetylsalicylic acid (99%) was purchased from Sigma-Aldrich (Germany). Acetate buffer pH 4.5 was prepared using concentrate purchased from J.T.Baker (Netherlands), dissolved with deionized and degassed water. Acetonitrile (HPLC grade) was purchased from Merck (Germany). Sodium lauryl sulphate (SLS) was obtained from Stanlab (Poland). Ezetimibe was dried by heating in an oven at 100 °C. After slow cooling, the samples of dehydrated EZT were stored in the desiccator at room temperature until further use.

Binary mixtures preparation

Most common method utilised to prepare solid dispersion is fusion method [26–28]. However, thermostability of

ingredients is basic condition of using this method [29]. Thus, to avoid the risk of aspirin thermal degradation, EZT–ASA solid dispersions were prepared by grinding method. The appropriate quantities of each component were weighed using a Sartorius microbalance (± 0.01 mg) and next grinded together in an agate mortar for about 10 min. Finely pulverized mixtures were then sieved using a 315-μm mesh size sieve. The prepared solid dispersions have been hermetically closed in glass vials and kept in a desiccator (at room temperature) until use. Nine EZT–ASA solid dispersions with mass percentages (mass%) of EZT of 10.0, 20.0, 30.0, 40.0, 50.0, 60.0, 70.0, 80.0 and 90.0 were prepared.

Particle size distribution (PSD) measurements

The particle size distribution (PSD) measurements were carried out by dynamic light scattering (DLS) method using ultrapure water as a dispersant. The Mastersizer 3000 (Malvern Instruments, UK) apparatus equipped with a HydroEV wet dispersion unit was used. Measurements were taken for representative mixtures containing 10, 50 and 90 mass% EZT. Approximately 0.1 g of powder was dispersed in 10 mL ultrapure water and shaken on vortex shaker in order to obtain homogenous suspension. An adequate amount of suspension was injected into a sample unit, filled with 800 mL of ultrapure water, until an ideal obscuration (10–20%) was achieved. The measurements rounds were conducted six times in the same conditions to obtain an average hydrodynamic diameter and size distribution.

Drug content

A quantity of 10 mg of each obtained mixture was dissolved in 100 mL of ethanol. The received solutions were filtered and content of EZT and ASA was determined by HPLC method, within the standard curves range from 5.0 to 50.0 μg mL^{-1}.

Thermal analysis

Thermal characterization of pure components and obtained mixtures was carried out using a heat flux-type DSC 214 Polyma (Netzsch, Germany). The calorimeter was equipped with the Intracooler 70 cooling accessory. The measuring device was calibrated for temperature and enthalpy using In (156.6 °C), Sn (231.9 °C), Bi (271.4 °C) and Zn (419.5 °C) as standards [30]. Measurement control and data analysis were performed with the use of Proteus® software (Netzsch, Germany). Samples for DSC measurements, with the mass about 4–6 mg, were weighed using a Sartorius microbalance (± 0.01 mg) in 40 μL Al crucibles and next sealed using punched lid. The same type of empty crucible was employed as a reference. The DSC scans were run in triplicate with a

heating rate of 5 °C min^{-1} in the temperature range from 25 °C to 180 °C. During measurements, a stream of inert gas (N$_2$, purity 99,999%) flowed through the DSC chamber at a rate of 25 mL min^{-1}. The DSC tests were conducted for all dispersions obtained as well as for pure components.

X-ray powder diffractometry

The X-ray powder diffraction (XRPD) studies were performed in order to identify phases present in the tested samples. XRPD patterns were collected at room temperature using a D2 Phaser (Bruker AXS, Germany) diffractometer operating in the 2θ mode with a horizontal goniometer, equipped with a LYNXEYE detector and CuKα radiation source (30 kV, 10 mA). The diffractometer was calibrated with a corundum sample supplied by Bruker AXS. Solid samples were placed into a low-background holder and scanned over 2θ range of 5° to 40° with a step size of 0.02°. The XRPD patterns were analysed using the Diffrac.Eva V 3.2 software.

Fourier transform infrared spectroscopy (FTIR)

The FTIR spectra were recorded on a Nicolet iS50 FTIR (Thermo Scientific, USA) spectrometer using an attenuated total reflection (ATR) mode with diamond crystal and evaluated by the OMNIC software version 5.0. The FTIR spectra were recorded using small amounts of the solid samples directly transferred to the ATR device compartment. The FTIR spectra were obtained as an average of accumulation of 32 scans per sample, registered in wavenumber range from 4000 to 400 cm^{-1} with a resolution of 4 cm^{-1}.

Scanning electron microscopy (SEM)

Particle morphology was examined on scanning electron microscope Zeiss EVO MA25. In order to increase the conductivity of the electron beam, all the samples were coated with gold and palladium (60:40; sputter current, 40 mA; sputter time, 50 s) using a Quorum machine (Quorum International, USA).

Dissolution tests

Dissolution tests were performed for all of the prepared solid dispersions as well as for pure components (EZT and ASA). Release studies were carried out in a USP type 2 (paddle) apparatus SR-8 Plus (Hanson Research, USA). The samples were determined by HPLC Ultimate 3000 Dionex (Thermo Fisher Scientific, USA) separation module using an UV–VIS DAD-type detector. The powder sample of each binary mixture as well as pure APIs in an amount of 20 mg was placed to 500 mL of dissolution medium and stirred at 50 rpm at

37 ± 0.5 °C. The pH 4.5 acetate buffer with 0.45% SLS was used as medium recommended by the US Pharmacopoeia for dissolution tests of ezetimibe tablets [31]. The solution samples were withdrawn at 5, 10, 20, 30, 40, 50 and 60 min by means of automatic sampler, filtered (0.20 μm pore size) and eluted with a phosphate buffer (pH 3.15): acetonitrile mobile phase at the ratios of 58:42 (v:v), respectively. The HPLC analysis was performed by isocratic elution with a flow rate of 0.6 mL min^{-1}, using a Purospher RP-18 column (125 cm × 3 mm, 5 μm, Merck). The APIs eluted from the column were identified by DAD detector at 230 nm. External standards of EZT and ASA were used to plot calibration curves. Linear calibration curves were obtained in the range of 5–50 μg mL^{-1} for both compounds (linearity $r^2 = 0.9999$).

Results and discussion

Drug content

EZT and ASA contents of the mixtures were found to be in the range of 97.4% to 101.9% and 97.7% to 101.8% of the declared EZT and ASA amount, respectively. Table 1 presents results of APIs content studies in prepared mixtures.

### Phase transition studies in the ezetimibe–aspirin system

Differential scanning calorimetry was used to determine the phase transitions of the pure components ASA and EZT, as well as to describe the binary system EZT–ASA. The DSC curves recorded for both APIs and investigated dispersions are presented in Fig. 1. The experimentally determined temperatures and enthalpies of phase transitions observed on DSC curves are shown in Table 2. EZT and ASA show a characteristic single endotherm peak ($\Delta H = 106.7$ J g^{-1} and $\Delta H = 176.5$ J g^{-1}, respectively)

Table 1 APIs content in prepared EZT–ASA mixtures

Composition/mass% EZT	Average content	
	EZT/%	ASA/%
10.0	100.3 ± 0.1	97.7 ± 0.4
20.0	98.5 ± 0.1	101.8 ± 0.1
30.0	98.4 ± 0.3	100.9 ± 0.1
40.0	98.8 ± 0.1	101.3 ± 0.1
50.0	101.9 ± 0.2	99.5 ± 0.2
60.0	97.4 ± 0.2	101.2 ± 0.1
70.0	98.6 ± 0.2	100.5 ± 0.1
80.0	98.9 ± 0.1	99.3 ± 0.2
90.0	97.5 ± 0.3	101.6 ± 0.2

Data expressed as mean $\pm$ SD (n = 3)

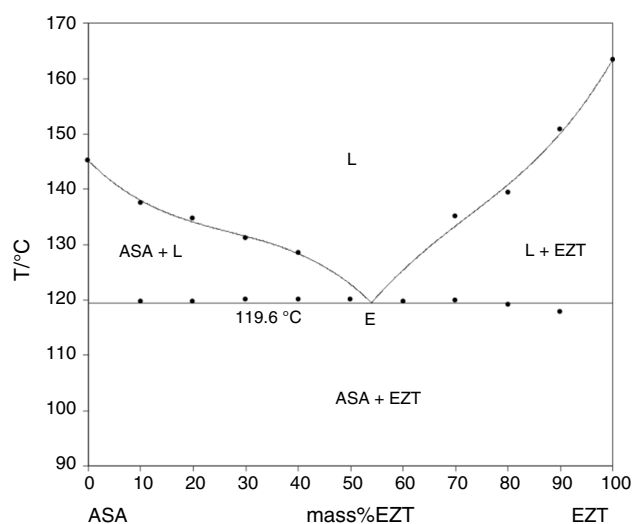Fig. 1 DSC curves of ASA, EZT and all obtained EZT–ASA solid dispersions
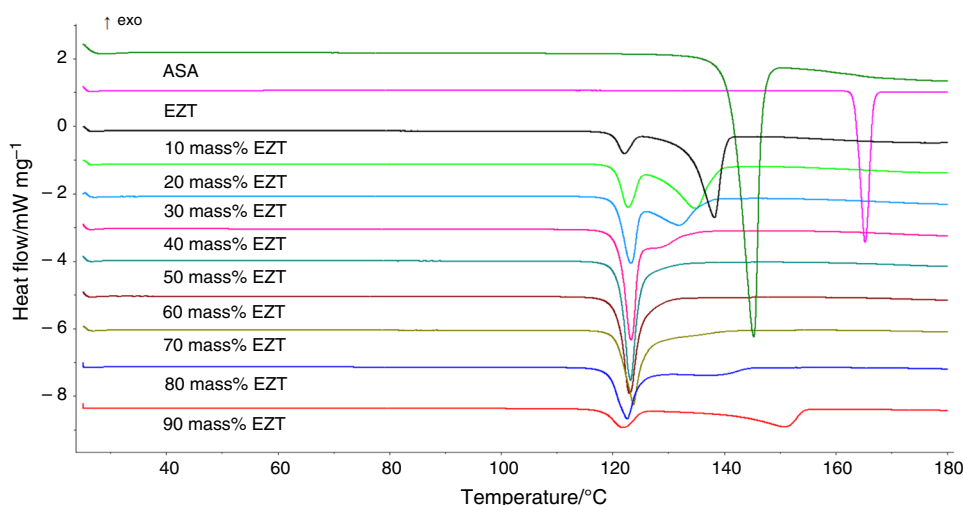
Table 2 Experimental temperature and enthalpy values for transitions observed in the EZT–ASA system

Composition/ mass% EZT	Eutectic invariant		Liquidus/°C
	Temperature/°C	ΔH/J g^{-1}	
0			145.3 ± 0.1
10.0	119.7 ± 0.1	19.40 ± 0.70	137.1 ± 0.1
20.0	120.0 ± 0.2	39.97 ± 0.91	134.1 ± 0.3
30.0	120.0 ± 0.3	61.67 ± 0.83	131.4 ± 0.2
40.0	120.2 ± 0.2	85.41 ± 0.81	128.5 ± 0.1
50.0	120.1 ± 0.3	106.80 ± 0.65	
60.0	119.8 ± 0.2	95.33 ± 0.82	
70.0	119.9 ± 0.1	77.76 ± 0.73	135.1 ± 0.4
80.0	119.2 ± 0.1	52.59 ± 0.61	139.5 ± 0.4
90.0	117.8 ± 0.3	23.80 ± 0.62	150.8 ± 0.5
100			163.5 ± 0.2

Data expressed as mean $\pm$ SD ($n = 3$)

Fig. 2 The EZT–ASA phase diagram determined on the DSC results analysis

corresponding to melting points at 163.5 °C and 145.3 °C, respectively. These values are close to those established previously for ezetimibe ($\Delta H = 94.2$ J g^{-1}, 164.4 °C) [32] and aspirin ($\Delta H = 167.6$ J g^{-1}, 141.0 °C) [33]. The DSC curves of the ASA–EZT mixtures clearly indicated that ASA and EZT formed a binary simple eutectic system. Figure 2 presents the EZT–ASA phase diagram constructed on the basis of the DSC results that compiled in Table 2. The DSC curves recorded for the samples of various dispersions (Fig. 1) demonstrated two endothermal effects with the characteristic outline for a simple eutectic system. As shown in Fig. 1, the first endothermal peak with a variable area has been appeared for all the dispersions at the same onset temperature. The second one was wider and depending on the mass ratio of EZT had a different maximum position. The onset of the first event indicates the temperature of an eutectic reaction 119.6 °C,

which follows the equation: solid acetylsalicylic acid (ASA) + solid ezetimibe (EZT) = liquid (L). This endothermic peak corresponding to the eutectic reaction is visible on the DSC curves recorded for all dispersions examined (Fig. 1). The values of the eutectic melting enthalpy ΔH (J g^{-1}) were determined by automatic integration of the eutectic peak area, which was estimated by subtraction of area corresponding to the complete liquefaction, using an optimal selection of integration line in Proteus® software. The obtained values are plotted in Fig. 3 versus mass ratio of EZT in order to construct Tamman's triangle [34, 35]. The maximum value of eutectic melting enthalpy has been estimated for 53.5 mass percentage of EZT and corresponds to the eutectic point (E) presented on the EZT–ASA phase diagram (Fig. 2). The enthalpy of the eutectic transition (Fig. 3) falls to zero for pure EZT and
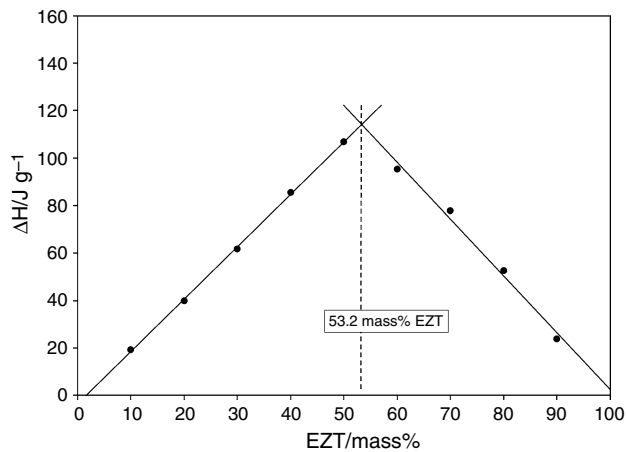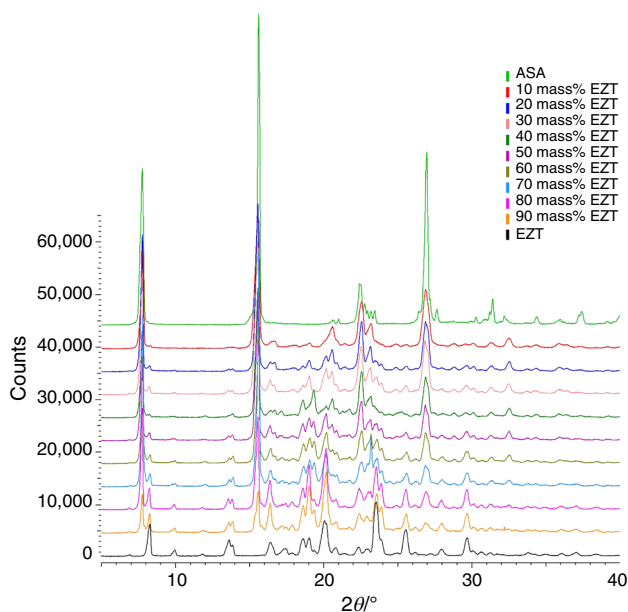
Fig. 3 Dependence of eutectic melting enthalpy ΔH on EZT mass ratio in the EZT–ASA system (Tamman's triangle construction)

ASA. This excludes formation of terminal solid solutions at either side of the EZT–ASA phase.

XRPD studies

The powder X-ray diffraction patterns of EZT, ASA and solid dispersion received by the grinding method are depicted in Fig. 4. Several distinct peaks can be observed at 2θ diffraction angles 7.77°, 15.62° and 26.97° for ASA and also 8.2°, 13.6°, 13.8°, 16.4°, 18.6°, 19.0°, 20.1°, 22.3°, 23.5°, 25.5°, 28.0° and 29.7° for EZT, indicating their

crystalline nature. These XRD reflections characteristics for ASA and EZT were also observed at the same angular positions in the analysed EZT–ASA solid dispersion patterns. Furthermore, no other reflections than those which are characteristic to pure ASA and EZT were observed on the patterns registered for the EZT–ASA mixtures. The registered reflection patterns show that no other crystallographically distinct phase was formed during the grinding process. These data indicate an absence of chemical interactions between the dispersion components in the solid state at room temperature. Furthermore, XRPD studies have shown that mixtures does not became amorphous and friction force acting on EZT and ASA particles during grinding has not caused polymorphic transitions.

FTIR studies

A series of FTIR experiments was performed in order to confirm or exclude the specific chemical interactions between both mixed drugs. The FTIR spectra of EZE, ASA and its solid dispersions samples recorded in the range of 4000 to 400 cm⁻¹ are presented in Fig. 5. The FTIR spectrum registered for pure EZT showed characteristic bands at: 3430 cm⁻¹ and 3265 cm⁻¹ (O–H stretching vibration), 1725 cm⁻¹ (C=O β-lactam stretching vibration), 1507 cm⁻¹ (benzene ring C=C stretching vibration), 1212 cm⁻¹ (C–F stretching vibration), 1063 cm⁻¹ (C–O stretching vibration) and 821 cm⁻¹ (para-substituted benzene ring vibration), which are consistent with the literature data [7]. The

Fig. 4 X-ray diffraction patterns of ASA, EZT and EZT–ASA solid dispersions with different mass ratio (mass%) of EZT
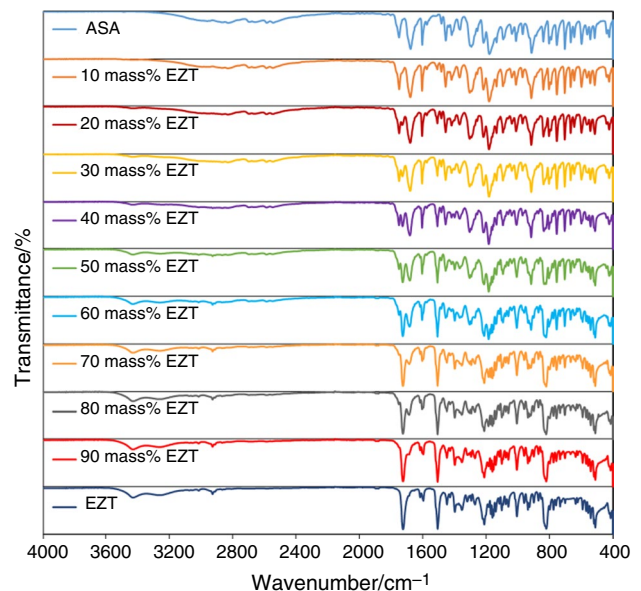

Fig. 5 FTIR spectra of pure components (ASA, EZT) and EZT–ASA solid dispersions with different mass ratio (mass%) of EZT

FTIR spectra registered for pure ASA showed characteristic absorption bands related to: acid C–O vibrations at 1217 cm^{-1}, benzene ring C=C stretching vibration at 1604 cm^{-1}, aliphatic C=O vibrations at 1678 and 1751 cm^{-1} and carboxylic acid O–H group stretching (a broad band at 2500–3500 cm^{-1}) which are also consistent with the literature data [36]. FTIR spectroscopy suggests that preparation of EZT–ASA solid dispersion by grinding method does not lead to interactions. All the major bands corresponding to the characteristic functional groups from EZT and ASA are observed in the FTIR spectres of the solid dispersions. The FTIR spectra of EZT–ASA solid dispersions demonstrate only a decrease in intensity of bands as compared to the FTIR spectra of pure ASA and EZT.

Scanning electron microscopy

SEM photomicrographs obtained in the magnification of 1000 for pure EZT, ASA and selected EZT–ASA solid dispersions are shown in Fig. 6. It can be seen on the presented micrographs that pure EZT and ASA formed block-shaped crystals. SEM photomicrographs registered for samples of binary EZT–ASA mixtures prepared by grinding show crystalline particles irregular in shape with significantly decreased size as a result of micronization. There were no major differences in particle morphology between the different EZT–ASA mixtures.
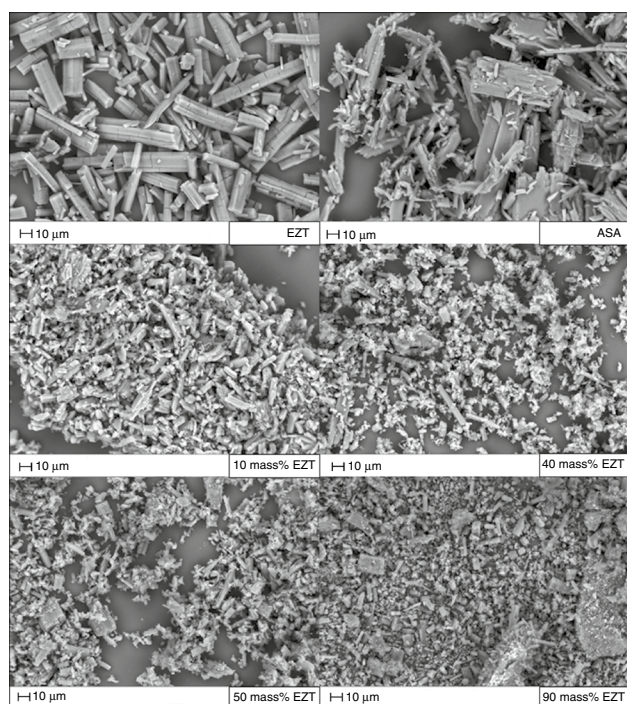
Fig. 6 SEM photomicrographs of EZT, ASA and selected EZT–ASA solid dispersions

Table 3 Particle size distribution results obtained by DLS method

Sample	Average diameter/μm		
	D_{10}	D_{50}	D_{90}
10 mass% EZT	0.85 ± 0.01	2.92 ± 0.05	7.87 ± 0.28
50 mass% EZT	0.88 ± 0.01	4.22 ± 0.04	15.00 ± 0.43
90 mass% EZT	0.86 ± 0.02	3.50 ± 0.02	11.00 ± 0.06
EZT	1.63 ± 0.03	6.67 ± 0.15	16.10 ± 0.45

Data expressed as mean $\pm$ SD ($n = 6$)

## Particle size distribution characteristic

The particle size characteristics are summarized in Table 3. The data obtained utilizing the DLS method correspond well with SEM analysis and clearly demonstrate that grinding method led to obtaining mixtures with particles diameter not exceeding 20 μm.

Dissolution studies

The activity of API is limited by its low solubility in water. Hence, the use of a suitable pharmaceutical system to enhance the apparent solubility and dissolution rate of the API would be highly desirable. The dissolution profiles achieved for 20 mg powder samples of each EZT–ASA binary mixtures are presented, respectively, in Fig. 7 for EZT and Fig. 8 for ASA. Our studies showed that the degree of EZT dissolution increases with the content of aspirin in the EZT–ASA mixture. The ezetimibe dissolution rate improvement was observed for solid dispersions containing from 40 to 90 mass% of ASA, which is the ingredient characterized by better water solubility [37]. This correlates with the phase diagram and indicates an improvement in EZT dissolution rate for all EZT–ASA mixtures that contains no more EZT than at the eutectic point (53.2 mass% EZT). The increase in dissolution rate of APIs forming simple eutectics is explained in the literature by decreasing particle size of both components which results in the increase in dissolution surface [38, 39]. In the EZT–ASA fixed-dose formulation, aspirin could be a second active ingredient as well as an effective carrier. As a crystalline carrier, ASA dissolves faster and effectively exposes the surface area of EZT fine crystals to wetting by solvent [40], affecting on ezetimibe release from binary solid dispersions. Thus, binary mixtures containing 10–60 mass% of EZT have achieved the main goal of enhancing the dissolution rate of EZT (the low water-soluble API coming under class II of BCS) in a fixed-dose system.

As shown in Fig. 7, almost 80% of the EZT have released from mixtures containing 10–30 mass% of EZT in 5 min, whereas only 25% has dissolved from pure sample of EZT.

Fig. 7 Dissolution profiles of EZT from their freeform and obtained EZT–ASA solid dispersions
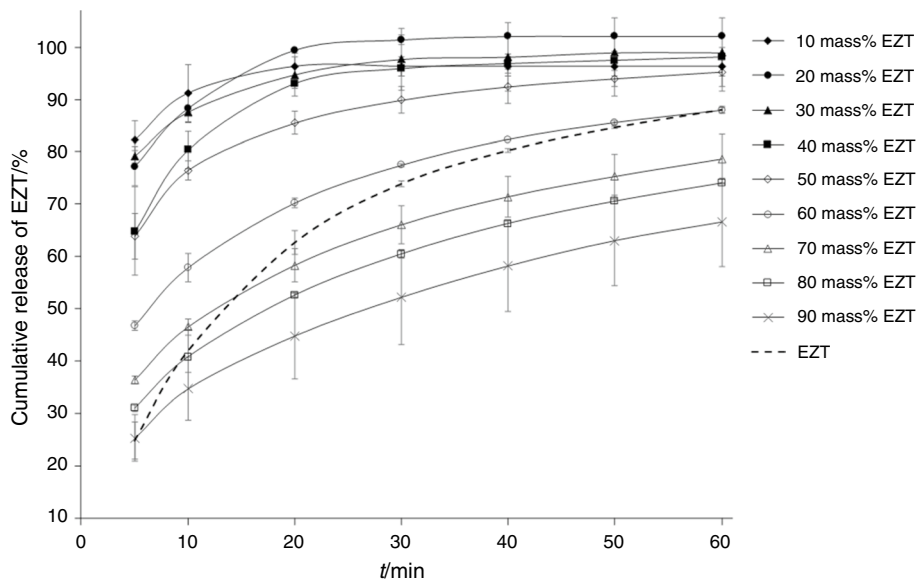
Fig. 8 Dissolution profiles of ASA from their freeform and obtained EZT–ASA solid dispersions
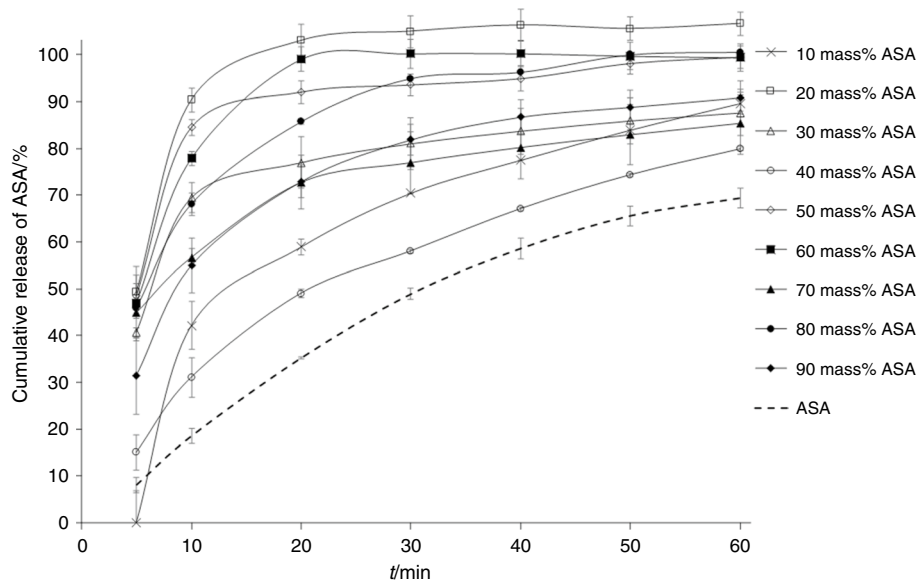
The ratios of 10 and 20 mass% EZT in the EZT–ASA mixtures are similar to the pharmacological dose ratios of EZT and ASA used in the cardiovascular disease therapy. If one considers the 10 mg EZT dose and ASA doses of 30–150 mg in the prevention of heart attack, the 10:90 and 20:80 of EZT–ASA solid dispersions with improved dissolution of APIs represent a desirable ratio of active ingredients.

Conclusions

Pharmaceutical eutectic mixtures are classified as a first-generation solid dispersion, consisting of active ingredient and crystalline carrier [40]. When eutectic mixtures are prepared by fusion method, the effective surface of fine crystals increases during fast simultaneous solidification of ingredients. The limitation of fusion method is that some drugs, e.g. aspirin, can be degraded by the melting process [26]. In this work, EZT–ASA solid dispersions were prepared by grinding. Grinding and milling are the basic and most common unit operations used in the drug form technology, generally

in order to reduce the particle size [41]. Our research clearly confirmed that simple grinding should not be disregard, as it can significantly act not only on particle size. Analysis of obtained DSC data has shown that simple grinding of two APIs can lead into formation of the eutectic mixture almost as effectively as simultaneous solidification of melted ingredients. Furthermore, XRPD studies have shown that mixtures remain crystalline and friction force acting on EZT and ASA particles during grinding has not caused polymorphic transitions. Dissolution studies of EZT–ASA system confirmed that the occurrence of eutectic in binary drug–drug mixtures prepared by grinding leads to an enhancing of solubility and dissolution rate of the ingredients, which may significantly affect the bioavailability of APIs in fixed-dose combinations. Since EZT and ASA doses are in the range of 10–20 mg and 75–162 mg [42], respectively, and the best released EZT–ASA mixtures contain 10–30 mass% of EZT, results of our studies make it possible the development of a single dosage form containing two APIs in a suitable therapeutic amount.

Compliance with ethical standards

Conflicts of interest The authors declare that they have no conflict of interest.

References

1. Roth GA, Forouzanfar MH, Moran AE, Barber R, Nguyen G, Feigin VL, Naghavi M, Mensah GA, Murray CJL. Demographic and epidemiologic drivers of global cardiovascular mortality. N Engl J Med. 2015;372:1333–411.
2. Nelson RH. Hyperlipidemia as a risk factor for cardiovascular disease. Prim Care. 2013;40:195–211.
3. Stone NJ, Robinson JG, Lichtenstein AH, Bairey Merz CN, Blum CB, Eckel RH, Goldberg AC, Gordon D, Levy D, Lloyd-Jones DM, Mc Bride P, Schwartz JS, Shero ST, Smith SC Jr, Watson K, Wilson PW. 2013 ACC/AHA guideline on the treatment of blood cholesterol to reduce atherosclerotic cardiovascular risk in adults: a report of the American College of Cardiology/American Heart Association Task Force on Practice Guidelines. Circulation. 2014;129:S1–S45.
4. Stewart J, Manmathan G, Wilkinson P. Primary prevention of cardiovascular disease: a review of contemporary guidance and literature. J R Soc Med Cardiovasc Dis. 2017;6:1–9.
5. Sleight P, Pouleur H, Zannad F. Benefits, challenges, and register-ability of the Polypill. Eur Heart J. 2006;27:1651–6.
6. Kolte D, Aronow WS, Banach M. Polypills for the prevention of cardiovascular diseases. Expert Opin Investig Drugs. 2016;25:1255–64.
7. Riekes MK, Engelen A, Appeltans B, Rombaut P, Stulzer HK, Van Den Mooter G. New perspectives for fixed dose combinations of poorly water-soluble compounds: A case study with ezetimibe and lovastatin. Pharm Res. 2016;33:1259–75.
8. Min KL, Park MS, Jung J, Chang MJ, Kim CO. Comparison of pharmacokinetics and safety of a fixed-dose combination of rosuvastatin and ezetimibe versus separate tablets in healthy subjects. Clin Ther. 2017;39:1799–810.
9. Knapik J, Wojnarowska Z, Grzybowska K, Jurkiewicz K, Tajber L, Paluch M. Molecular dynamics and physical stability of coamorphous ezetimib and indapamide mixtures. Mol Pharm. 2015;12:3610–9.
10. Sanz G, Fuster V, Guzmán L, Guglietta A, Arnáiz JA, Martínez F, Sarria A, Roncaglioni MC, Taubert K. The fixed-dose combination drug for secondary cardiovascular prevention project: improving equitable access and adherence to secondary cardiovascular prevention with a fixed-dose combination drug. Study design and objectives. Am Heart J. 2011;162:811–7.
11. Lestari MLAD, Ardiana F, Indrayanto G. Ezetimibe. Profiles Drug Subst Excip Relat Methodol. 2011;36:103–49.
12. Sudhop T, Lutjohann D, Kodal A, Tribble DL, Shah S, Perevozskaya I, Von Bergmann K. Inhibition of intestinal cholesterol absorption by ezetimibe in humans. Circulation. 2002;106:1943–8.
13. Nutescu EA, Shapiro NL. Ezetimibe: a selective cholesterol absorption inhibitor. Pharmacotherapy. 2003;23:1463–74.
14. Knopp RH, Gitter H, Truitt T, Bays H, Manion CV, Lipka LJ, LeBeaut AP, Suresh R, Yang B, Veltri EP. Effects of ezetimibe, a new cholesterol absorption inhibitor, on plasma lipids in patients with primary hypercholesterolemia. Eur Heart J. 2003;24:729–41.
15. Bove M, Fogacci F, Cicero AFG. Pharmacokinetic drug evaluation of ezetimibe + simvastatin for the treatment of hypercholesterolemia. Expert Opin Drug Metab Toxicol. 2017;13:1099–104.
16. Saxon DR, Eckel RH. Statin intolerance: a literature review and management strategies. Prog Cardiovasc Dis. 2016;59:153–64.
17. Hammersley D, Signy M. Ezetimibe: an update on its clinical usefulness in specific patient groups. Ther Adv Chronic Dis. 2017;8:4–11.
18. Berger JS, Brown DL, Becker RC. Low-dose aspirin in patients with stable cardiovascular disease: a meta-analysis. Am J Med. 2008;121:43–9.
19. Ittaman SV, VanWormer JJ, Rezkalla SH. The role of aspirin in the prevention of cardiovascular disease. Clin Med Res. 2014;12:147–54.
20. Górniak A, Wojakowska A, Karolewicz B, Pluta J. Phase diagram and dissolution studies of the fenofibrate—acetylsalicylic acid system. J Therm Anal Calorim. 2011;104:1195–200.
21. Górniak A, Karolewicz B, Żurawska-Płaksej E, Pluta J. Thermal, spectroscopic, and dissolution studies of the simvastatin—acetylsalicylic acid mixtures. J Therm Anal Calorim. 2013;111:2125–32.
22. Górniak A, Gajda M, Pluta J, Czapor-Irzabek H, Karolewicz B. Thermal, spectroscopic and dissolution studies of lovastatin solid dispersions with acetylsalicylic acid. J Therm Anal Calorim. 2016;125:777–84.

23. Barkas F, Liberopoulos E, Elisaf M. Impact of compliance with antihypertensive and lipid-lowering treatment on cardiovascular risk benefits of fixed-dose combinations. Hell J Atheroscler. 2013;1:18–25.

24. Bruni G, Sakaj M, Berbenni V, Maggi L, Friuli V, Girella A, Milanese Ch, Marini A. Physico-chemical and pharmaceutical characterization of sulindac–proglumide binary system. J Therm Anal Calorim. 2019;136:2063–70.

25. Dichi E, Sghaier M, Guiblin N. Reinvestigation of the paracetamol–caffeine, aspirin–caffeine, and paracetamol–aspirin phase equilibria diagrams. J Therm Anal Calorim. 2018;131:2141–55.

26. Vasconcelos T, Sarmento B, Costa P. Solid dispersions as a strategy to improve oral bioavailability of poor water soluble drugs. Drug Discov Today. 2007;12:1068–75.

27. Shamsuddin MF, Shahid HA, Javed A. Development and evaluation of solid dispersion of spironolactone using fusion method. Int J Pharm Investig. 2016;6:63–8.

28. Hallouard F, Lahiani-Skiba M, Anouard Y, Skiba M. Solid dispersions for oral administration: an overview of the methods for their preparation. Current Pharm Design. 2016;22:1–17.

29. Meng F, Gala U, Chauhan H. Classification of solid dispersions: correlation to (i) stability and solubility (ii) preparation and characterization techniques. Drug Dev Ind Pharm. 2015;41:1401–15.

30. Della Gatta G, Richardson MJ, Sarge SM, Stølen S. Standards, calibration, and guidelines in microcalorimetry. Part 2. Calibration Standards for Differential Scanning Calorimetry (IUPAC Technical Report). Pure Appl Chem. 2006;78:1455–76.

31. USP 41-NF 36 S2, 2018, United States Pharmacopeial Convention; Rockville, USA

32. Sugandha K, Kaity S, Mukherjee S, Isaac J, Ghosh A. Solubility enhancement of ezetimibe by a cocrystal engineering technique. Cryst Growth Des. 2014;14:4475–86.

33. Perlovich GL, Kurkov SV, Kinchin AN, Bauer-Brandl A. Solvation and hydration characteristics of ibuprofen and acetylsalicylic acid. AAPS Pharm Sci. 2004;6:1–9.

34. Rycerz L. Practical remarks concerning phase diagrams determination on the basis of differential scanning calorimetry measurements. J Therm Anal Calorim. 2013;113:231–8.

35. Marinescu DC, Pincu E, Oancea P, Bruni G, Marini A, Meltzer V. Solid-state study of captopril and metoprolol tartrate binary system. J Therm Anal Calorim. 2015;120:829–37.

36. Tita D, Jurca T, Fulias A, Marian E, Tita B. Compatibility study of the acetylsalicylic acid with different solid dosage forms excipients. J Therm Anal Calorim. 2013;112:407–19.

37. Dressman JB, Nair A, Abrahamsson B, Barends DM, Groot DW, Kopp S, Langguth P, Polli JE, Shah VP, Zimmer M. Biowaiver monograph for immediate-release solid oral dosage forms: acetylsalicylic acid. J Pharm Sci. 2012;101:2653–67.

38. Leuner C, Dressman J. Improving drug solubility for oral delivery using solid dispersions. Eur J Pharm Biopharm. 2000;50:47–60.

39. Goud NR, Suresh K, Sanphui P, Nangia A. Fast dissolving eutectic compositions of curcumin. Int J Pharm. 2012;439:63–72.

40. Kim KT, Lee JY, Lee MY, Song ChK, Choi J, Kim DD. Solid dispersions as a drug delivery system. J Pharm Investig. 2011;41:125–42.

41. Loh ZH, Samanta AK, Heng PWS. Overview of milling techniques for improving the solubility of poorly water-soluble drugs. Asian J Pharm Sci. 2015;10:255–74.

42. Godley RW, Hernandez-Vila E. Aspirin for primary and secondary prevention of cardiovascular disease. Tex Heart Inst J. 2016;43:318–9.